JX-ISAS-SUZAKU-MEMO-2010-07
Title: Result of On-board Experiments of Increased Amount of Charge Injection for XIS1
Category: XIS
Author: M. Tsujimoto (ISAS), E. D. Miller (MIT), H. Murakami (Rikkyo), H. Matsumoto (Nagoya), H. Takahashi, K. Hayashida (Osaka), M. Sawada, S. Nakashima, M. Nobukawa (Kyoto)
Date: 2011-06-24 Version: 4

Summary

Context: The XIS onboard Suzaku has proven that charge injection (CI) is quite effective to rejuvenate the performance of X-ray CCD detectors, which are subject to rapid degradation in the orbit under a constant dosage of cosmic-ray radiation. Since we started the CI operation in 2006, the rate of decrease in the charge transfer efficiency has been markedly alleviated. The rate is, however, larger for the back-illuminated (BI) sensor (XIS1) than the other front-illuminated (FI) sensors (XIS0, 2, 3), because we decided to inject less amount of charges (2 keV equivalent) for the BI sensor than the FI sensors (6 keV equivalent) so as not to sacrifice its superior low energy performance.
Aims: We revisit the decision made in 2006 in response to the performance changes since then. We examine if increasing CI amount to 6 keV equivalent for the BI sensor has scientific merits as of 2010.
Method: We conducted a series of observations with 2 vs 6 keV equivalent charges for selected targets, compared the improvements, and identified possible drawbacks by the change.
Results: With the increased CI amount, we found that the high-energy response has improved prominently with a negligible loss in the low-energy performance. We encountered a significant telemetry saturation, however, due to the leakage of injected charges during the charge transfer. Therefore, we installed a new μ-code to mask these artificial events. The XIS1 operation with the new μ-code was started on 2011-06-01 for the Normal mode, which will be followed by the Normal mode with window/burst options. The gain and resolution for new data will be changed significantly, requiring the release of new CALDB. Data taken with CI=6 keV shall not be processed with the old calibration constructed with CI=2 keV. Users are advised to follow the latest announcements from the XIS team.

1 Background

The X-ray Imaging Spectrometer (XIS) is an X-ray instrument onboard the Suzaku satellite, which is in operation for 5.5 years. The XIS is equipped with four X-ray CCD devices (XIS0–3) capable of imaging-spectroscopic observations at a 0.2–12 keV energy range with a moderate energy resolution of R ~30–50. Three CCDs are front-illuminated (FI) devices (XIS0, 2, and 3), while the remainder is a back-illuminated (BI) device (XIS1). The FI and BI sensors are superior to each other in the high and low energy response, respectively.

X-ray CCD devices are subject to degradation in the orbit. One of the outcomes is the increase of charge traps under constant radiation in the space environment. This results in the decrease in the charge transfer efficiency (CTE), which leads to the degradation in the energy resolution.

The XIS has a function to precisely monitor and mitigate this effect. For monitoring, each sensor has ^{55}Fe calibration sources at two corners in the far-side of the readout. For mitigation, charge injection (CI) is implemented. Electrons are injected artificially from one side of the chip and are read out along with charges produced by X-ray events. Artificial charges are injected periodically in space (one in 54 rows), which fill in charge traps sacrificially, and thereby alleviate the decrease in the CTE for charges by X-ray events.

Fig. 1 shows the long-term trend of the measured peak energy and width of the Mn I Kα line (5.9 keV) from the ^{55}Fe calibration sources. The CI technique was put into routine operation since the

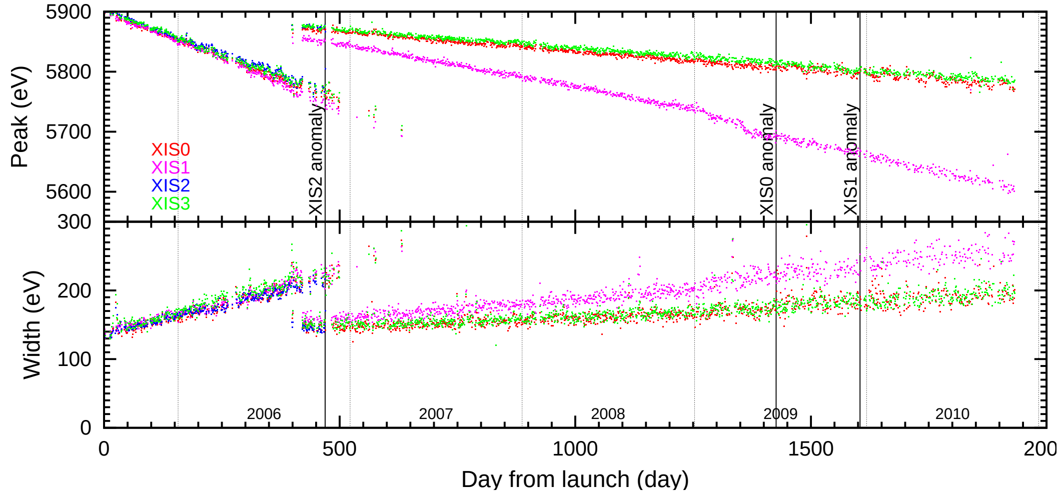

Figure 1: Trend of peak energy and width of Mn I Kα emission from ^{55}Fe calibration source.

middle of 2006 and has brought a drastic improvement. At the start of the CI operation, the XIS team decided to inject the amount of charges equal to the amount produced by a 6 keV X-ray photon ("6 keV equivalent") for the FI devices and a smaller amount ("2 keV equivalent") for the BI device. The smaller amount is due to the expected increase in noise in the low energy end of the spectrum, at which the BI device has an advantage over the FI device.

The situation has changed since then. The accumulation of the contaminating material on the surface of the CCDs made the low-energy advantage of the XIS1 less prominent. The CTE for the BI device decreases at a faster rate. As a consequence, the astrophysically important lines of Fe XXV (6.7 keV) and Fe XXVI (7.0 keV) are no longer resolved. The XIS team revisited the 2006 decision and started to take steps to judge whether the CI increase to 6 keV equivalent is beneficial for XIS1.

In 2010, we conducted a series of onboard experiments to evaluate the performance improvements and possible side effects of the CI increase for the XIS1. This article summarizes the results and argue for the routine operation of the increased CI of 6 keV equivalent starting from the AO6 cycle.

2 Data Acquisition

Table 1 summarizes the data set obtained in the experiment. We mainly used E0102–72 and Cygnus Loop, super-nova remnants with a line-dominated soft emission, to measure the low-energy response, and the Perseus cluster, a cluster of galaxies with extended hard emission, to measure the high-energy response. We did not use ^{55}Fe data for the CI=2 vs 6 keV comparison because they are too weak to use within the limited telescope time allocation for XIS calibration observations.

3 Results

3.1 Image

Fig. 2 shows the frame dump images taken with the CI=4, 6, and 8 keV (data ID #1 in Table 1). All images appear healthy. The column-to-column variation is more apparent for smaller amount of CI.

3.2 High-energy response

High-energy response was checked with a comparison data set of data ID #5 and #6 (Table 1) using strong Fe XXV and Fe XXVI emission lines from the Perseus cluster. The emission is pervasive across

Table 1: Data set.

ID	Target name	Seq. number	Obs. date	$t_{\rm exp}$ (ks)	Comment
1	CYGNUS_LOOP_P8	105007010	2010-06-11	10	Frame dump w. CI=4, 6, 8 keV.
2	E0102-72	105004020	2010-06-19	20	CI=2 keV.
3	E0102-72_1_4_WIN	105005010	2010-06-19	20	CI=2 keV.
4	E0102-72_PSUM	105006010	2010-06-20	40	CI=6 keV. Data lost for DR overwritten.
5	PERSEUS	105009010	2010-08-09	30	CI=6 keV.
6	PERSEUS_1_4_WIN	105010010	2010-08-10	30	CI=2 keV.
7	E0102-72_PSUM	105006030	2010-08-29	40	CI=6 keV. Heavy telemetry saturation.
8	E0102-72	105004040	2010-10-26	20	CI=6 keV. Slight telemetry saturation.
9	E0102-72_PSUM	105006020	2010-12-07	40	CI=6 keV. Lower event thres = 35.
10	E0102	105004050	2010-12-09	20	CI=2 keV.
11	E0102_1_4_WIN	105005020	2010-12-09	20	CI=2 keV.
12	CYG_LOOP_P8_6	105007020	2010-12-22	5	CI=6 keV.
13	CYG_LOOP_P8_2	105007030	2010-12-23	5	CI=2 keV.
14	PERSEUS	105009020	2011-02-03	40	CI=2 keV.
15	PERSEUS_1_4_WIN	105010020	2011-02-02	20	CI=2 keV.
16	PERSEUS	105027010	2011-02-22	40	CI=6 keV.
17	PERSEUS_1_4_WIN	105028010	2011-02-21	20	CI=6 keV.

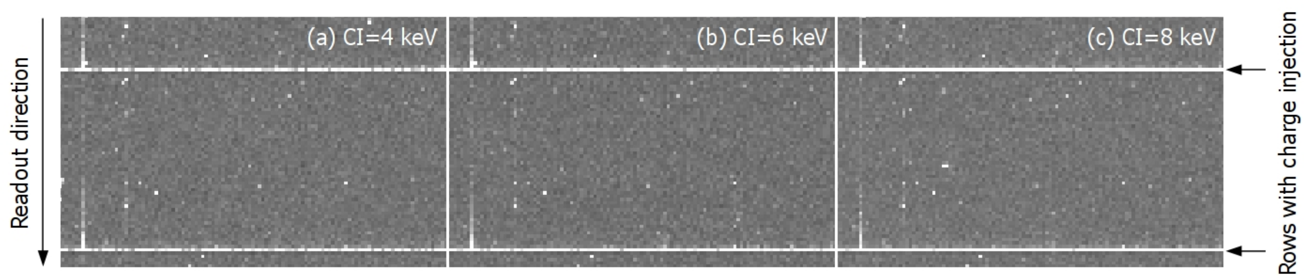

Figure 2: Enlarged view of frame dump images with different amount of CI.

the entire XIS1 field of view. Fig. 3 compares the result between CI of 2 vs 6 keV. The peaks are noticeably higher and narrower for the CI=6 keV data with a 33% improvement in the FWHM.

3.3 Low-energy response

Low-energy response was examined by comparing two E0102–72 (#9 and #10) and two Cygnus loop (#12 and #13) spectra. The E0102–72 spectra were accumulated from the central part of the CCD (segments B and C). Figure 4 shows the result of fitting by a phenomenological model of a power-law continuum (Γ for photon index and $N_{\rm PL}$ for normalization) plus numerous emission lines attenuated by the interstellar photoelectric absorption with a column of $N_{\rm H}$. The width of the lines were thawed collectively for all the lines. The width and the constant value for the entire spectrum were thawed independently for the CI=2 keV and 6 keV data, while other parameters were derived from the CI=6 keV spectrum and fixed for the CI=2 keV spectrum. The detector response of a zero width was used for this fitting. Table 2 summarizes the result, in which we see some improvements from the 2 keV to 6 keV data. However, this change is within data-to-data scatter in the long-term development of the data.

Likewise, the two Cygnlus loop spectra showed no significant differences between CI=2 and 6 keV. Figure 5 shows the comparison between the two. The fitting result by two bremmstrahling and three

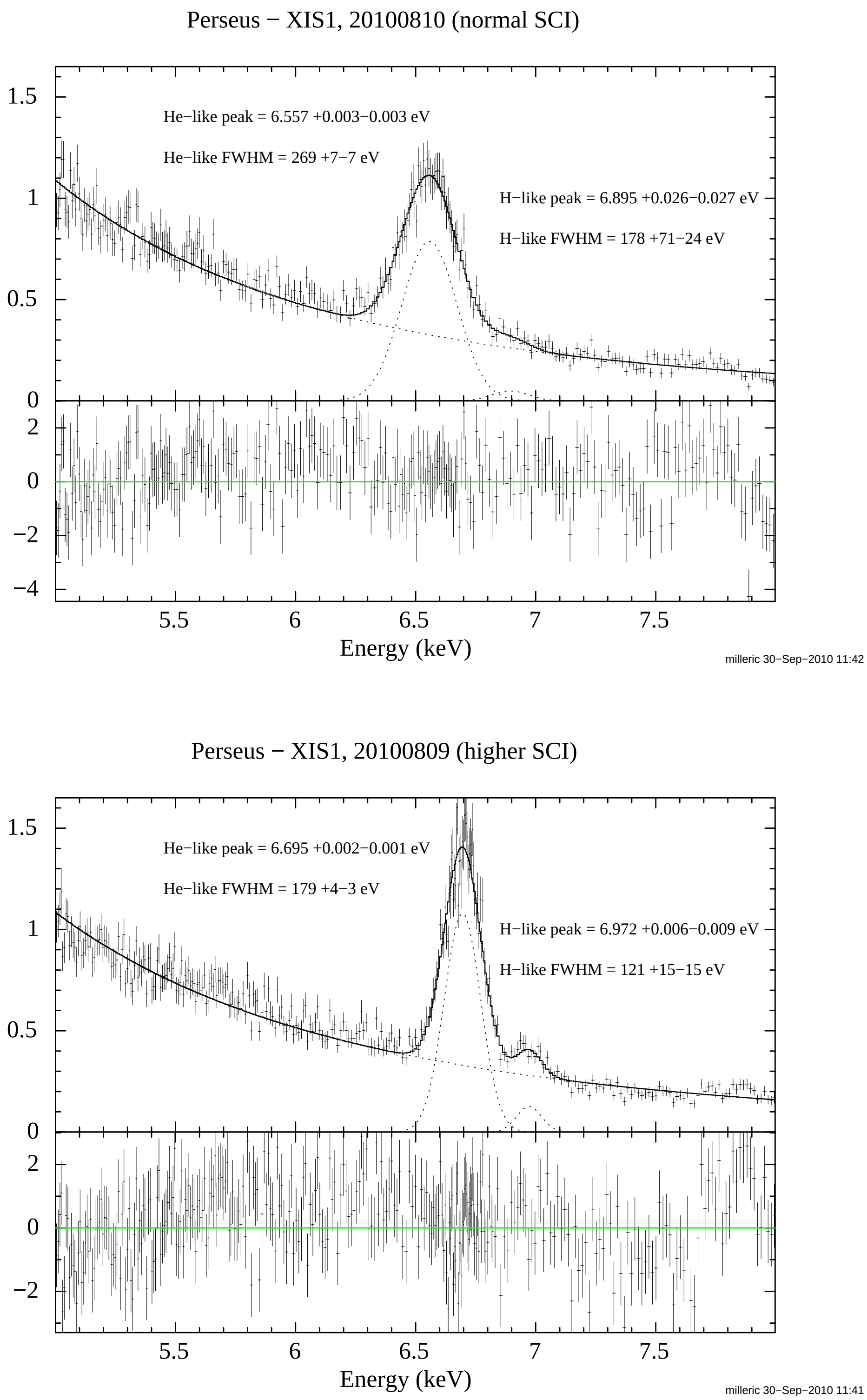

Figure 3: Comparison of Fe XXV and Fe XXVI lines from the Perseus cluster with the CI of 2 keV (top) and 6 keV (bottom).

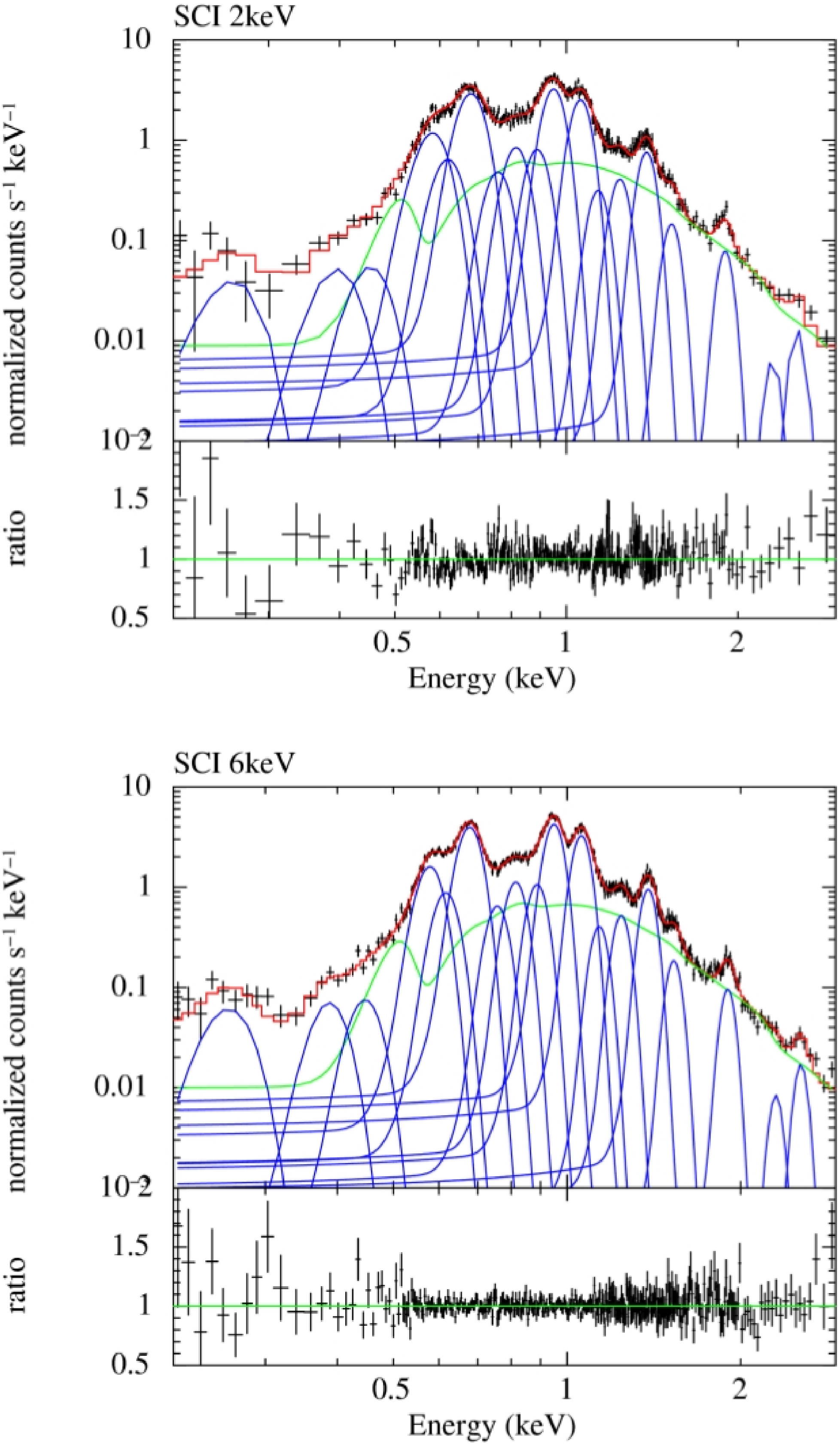

Figure 4: Result of fitting with a phenomenological model of the E0102–72 spectrum with the CI of 2 keV (top) and 6 keV (bottom).

Table 2: Fitting result of E0102–72 spectrum.

Parameter	Unit	CI=6 keV	CI=2 keV
Constant		1.0	0.89
$N_{\rm H}$	10^{21} cm^{-2}	5.6	5.6
Γ		5.3	5.3
$N_{\rm PL}$		1.2×10^{-2}	1.2×10^{-2}
σ	(eV)	1.5×10^{-2}	2.5×10^{-2}

Gaussian lines are consistent within the statistical uncertainty.

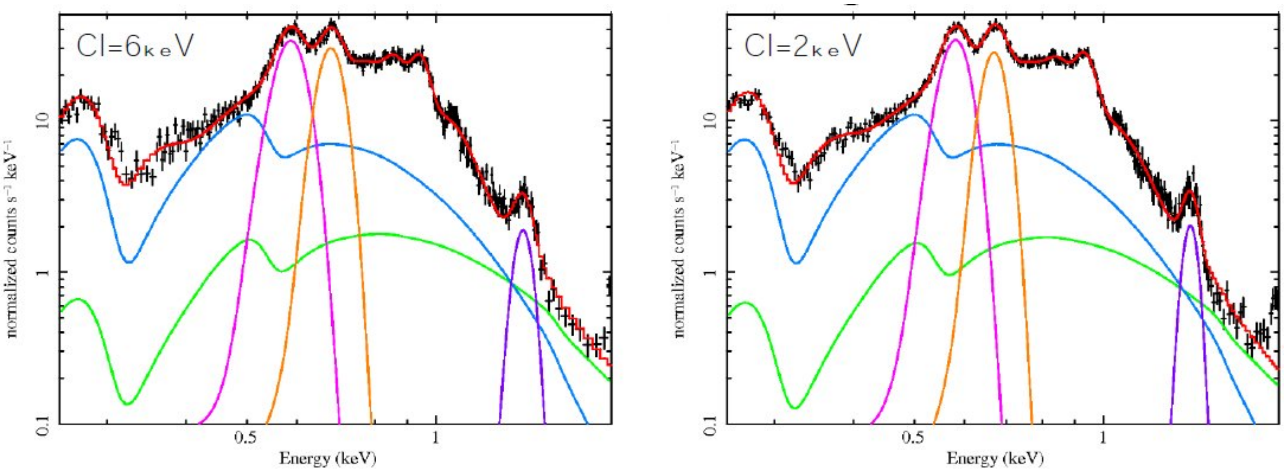

Figure 5: Result of fitting with a phenomenological model of the Cygnus loop spectrum with the CI of 2 keV (right) and 6 keV (left).

3.4 Telemetry saturation and countermeasures

We encountered a significant telemetry saturation while we were observing E0102–72 with CI=6 keV (data ID #7 and #8 in Table 1). This was caused by a combination of (a) reduced telemetry bandpass in weekends, (b) increased artificial events due to increased CI amounts, and (c) gradual increase in non X-ray background of XIS1.

Figure 6 shows the rate of telemetry and the elevation from the Earth are shown as a function of time for the data ID #8. The telemetry is saturated in some time intervals.

Figure 7 shows the rate of telemetry as a function of time separately for the night earth and day earth elevations. Even at high elevations, the data rate exceeds the telemetry limit, resulting in an effective loss of observing time. The loss is reduced by raising the low event threshold from 20 (left panel) to 35 (right panel), but this does not solve the issue completely. Further increase of low event threshold cannot be accommodated considering its scientific impact.

The increased telemetry is mostly due to leakage of injected charges. They are localized in the image behind the charge injection rows. A new set of μ-codes is being developed, which will solve the telemetry saturation problem by masking these artificial events onboard. The new codes will be implemented some time in the AO6 cycle. As of writing, a new code was installed and started to be used for the Normal mode operation since 2011-06-01.

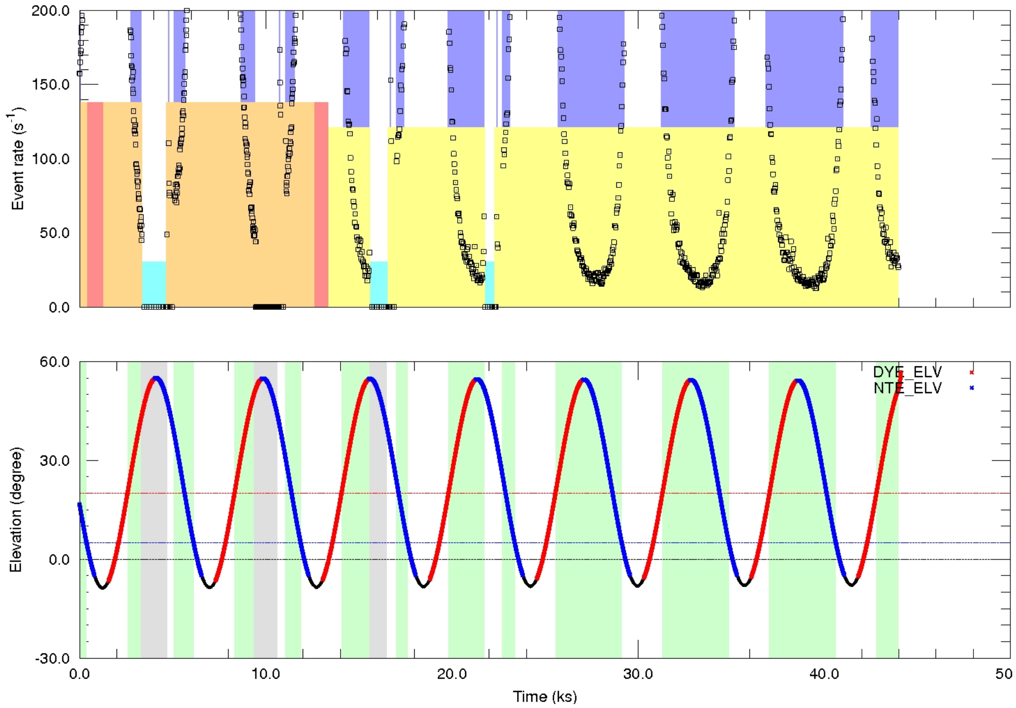

Figure 6: Telemetry rate (upper) and elevation from the Earth (bottom) as a function of time in the E0102–72 data taken with the CI amount of 6 keV on a week day. In the upper panel, the data rate is shown with different colors: red (super-high), orange (high), yellow (medium), and low (cyan). The hight of the bands indicates the telemetry limit. The time intervals of telemetry saturation are shown with blue bands above the limit. In the lower panel, the SAA is shown with grey, while the good time intervals by the standard screening criteria are shown with green bands.

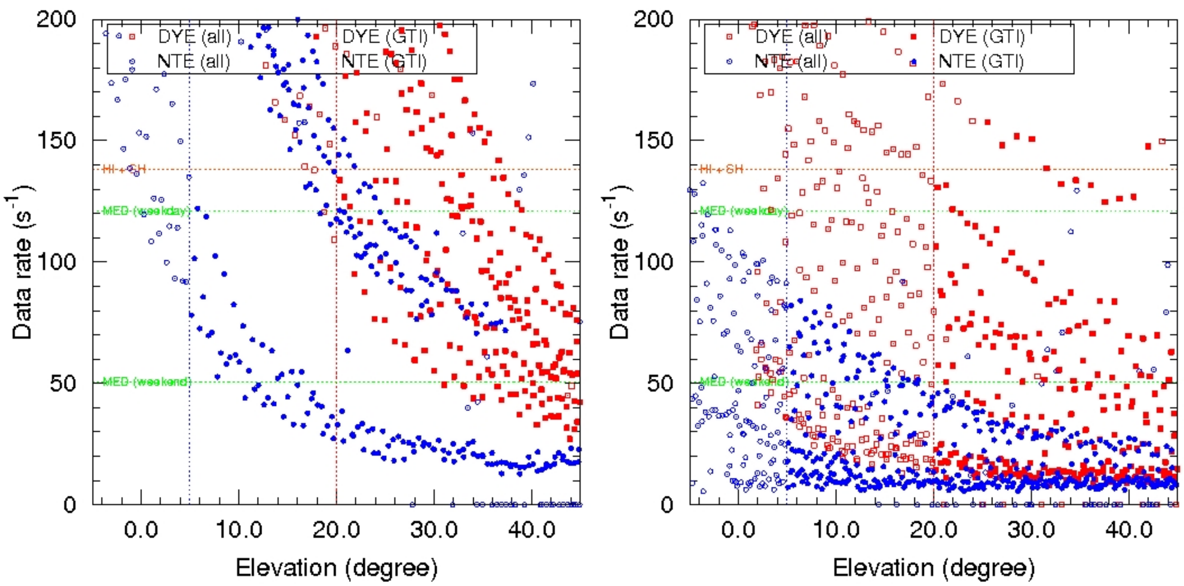

Figure 7: Telemetry rate as a function of elevation angle from the night and day Earth for CI=6 keV low event threshold of 20 (left, data ID #8) and 35 (right, data ID #9). The data in all times are shown with open symbols, while those only in the good time intervals with the standard screening criteria are shown with filled symbols.

4 Caution for Users

4.1 Data processing and new calibration data

As is seen in Fig. 3, the gain and energy resolution change drastically for the data with increased CI. The calibration information should be updated to accommodate these changes. The products by the pipeline processing version TBA and later and the CALDB version TBA and later shall be used to analyze CI=6 keV data.

It is expected to take some time to construct the new calibration database for CI=6 keV. This is because we need to follow the long-term trend of the XIS performance variation over many months. In the meanwhile, we will release an interim version of the calibration information as early as possible, which will be implemented in the pipeline processing and the CALDB.

4.2 Event screening

Because of the onboard masking of the events in rows behind the charge injection rows, there is a slight, though negligible, change in the data products.

In the XIS data processing, pixel qualities are given as a set of 32 flags for each event. Events detected one row behind the injection rows are given a flag of **SCI_TRAILING_ROW** (the 29th bit in the pixel quality) and those two rows behind the injection rows are given **SCI_2ND_TRAILING_ROW** (the 18th bit in the pixel quality; Fig. 8). In the standard processing, events in the second trailing rows are included, while those in the zeroth and the first trailing rows are discarded.[1]

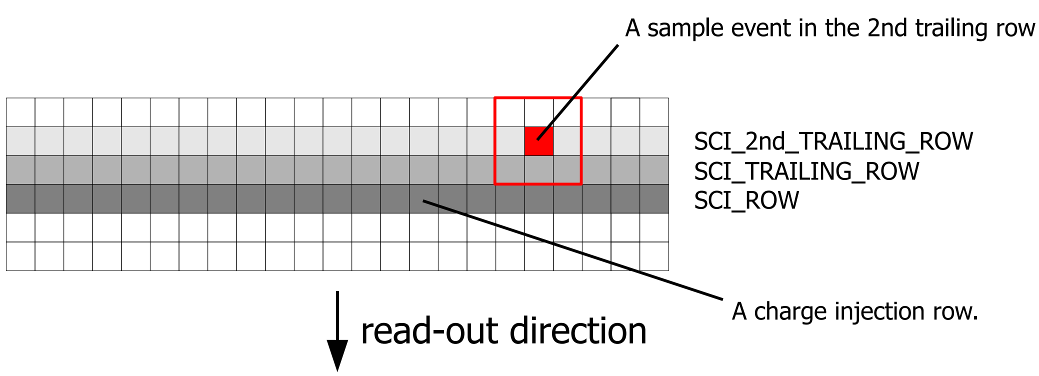

Figure 8: Flags for events behind the charge injection rows.

In the new μ-codes, all information in the first trailing rows are discarded onboard. Therefore, events detected in the second trailing row (a sample is shown by red in Fig. 8) do not have a complete set of information for grading and event reconstruction, which is based on the charge distribution over 3×3 pixels. In theory, this may change the redistribution matrix at the low energy end. However, this effect was confirmed to be almost negligible with real data (Fig. 9).

If you want to be precise, you can remove events in the second trailing rows by altering the standard screening criteria. You need to reprocess your event files and filter out events in the second trailing row using the `STATUS` column in the event file. The change should be consistent with the `pixq` parameter, which is referred by the `xissimarfgen`, `xisexpmapgen`, and `xisnxbgen` tools in the `FTOOLS` package. The default `pixq` parameter (designated as `pixq_min`=0, `pixq_max`=524287, `pixq_and`=65536, and `pixq_eql`=0) is set to be consistent with the standard processing criteria. For details of these parameters, please see the manuals of these tools.

[1]See http://www.astro.isas.jaxa.jp/suzaku/process/v2changes/criteria_xis.html for detail.

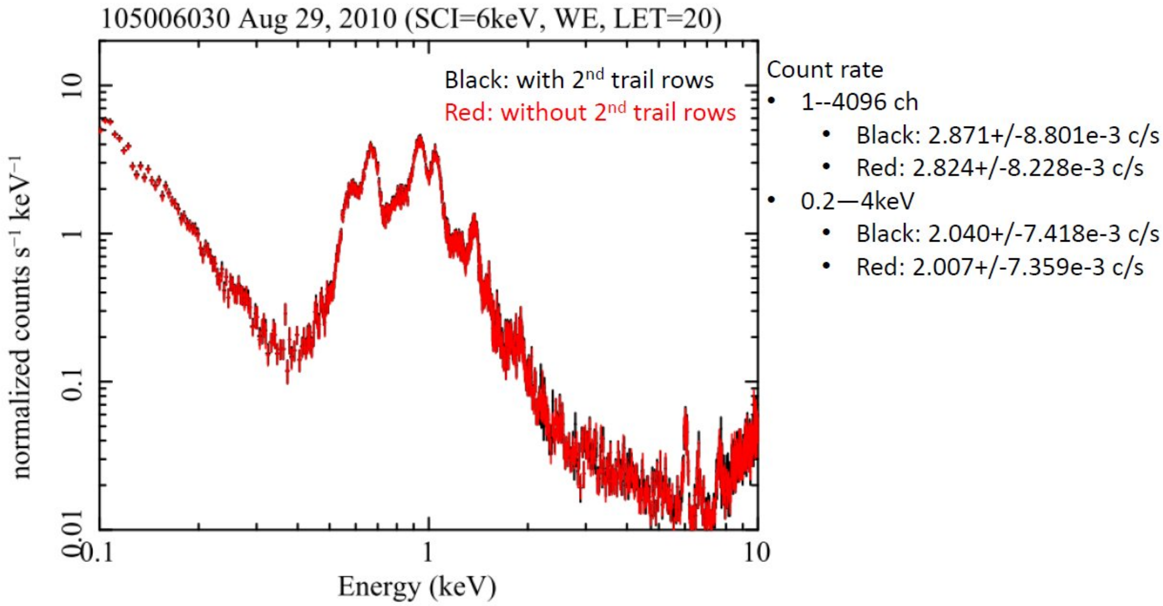

Figure 9: Comparison of E0102–72 spectra constructed from events including (black) and excluding (red) events detected in the second trailing rows.

5 Conclusion

With increased CI amount from 2 to 6 keV equivalent the response improves significantly both in the high-energy bands. The telemetry saturation is encountered, with can be solved by introducing a new μcode to mask the charge leakage. This will be put into operation some time during the AO6 period.

Data taken with the new CI setup require new pipeline processing and CALDB. These will be released some time during the AO6 period. Users need to check the versions of their products for their CI=6 keV data.

Events detected in the second row from the charge injection rows may not be precise in grading and event reconstruction. This effect, however, was found negligible in practice.